



Numerical modelling of sonic crystal noise barriers with absorbing scatterers

Matheus Duarte Veloso¹, Luís Godinho¹, Paulo Amado Mendes¹, Javier Redondo², Matheus Pereira³

¹ University of Coimbra, ISISE, Department of Civil Engineering, Coimbra, Portugal.

(matheus.veloso@student.dec.uc.pt, lgodinho@dec.uc.pt, pamendes@dec.uc.pt),

² Universitat Politècnica de València, Research Institute for the Integrated Management of Coastal Zones, València, Spain.

(fredondo@fis.upv.es)

³ University of Porto, Construct, Department of Civil Engineering, Porto, Portugal.

(pmatheus@fe.up.pt)

Abstract

Noise attenuation by sonic crystal noise barriers (SCNB) occurs mainly in specific frequency bands (band gaps), due to a mechanism called Bragg scattering, which is the result of destructive interference between multiple reflections. To improve their performance, sound-absorbing materials may be used coating the rigid scatterers, increasing attenuation in other frequency bands. In this work, the Method of Fundamental Solutions (MFS) is used to evaluate the performance of SCNB with cylinders covered by porous and granular materials considering two strategies: i) imposing the surface impedance (Z_s) of the absorbent material, at the collocation points of the numerical model; ii) simulating the volume of the absorbent material using equivalent fluid models for porous or granular materials. The proposed numerical models were verified and used to analyze the acoustic behavior of SCNB with absorbing scatterers and the enhancement of their mitigation effect with porous materials.

Keywords: SCNB, MFS, numerical model, equivalent fluid model, surface impedance.

1 Introduction

Acoustic barriers are commonly used when there are buildings that are located near roads and are exposed to high sound pressure levels. According to Gill [1], Hutchins et al. [2] and Bies and Hansen [3], the most convenient shape of an acoustic barrier is of the wall type, as it only has diffraction at the top of the barrier, since its length is considered infinite in relation to its height. The acoustic barriers' efficiency could be analysed in terms of Insertion Loss [4].

According to [5, 6, 7, 8], the interest in developing solutions such as sonic crystal barriers has been increasing for road traffic noise mitigation. In 1995, Martínez-Sala et al. [9] proved that the periodic distribution of wave disperses in three-dimensional spaces provides sound waves attenuation at specific frequency bands, forming the so-called acoustic band-gaps.

According to Martins [4], it was observed that the maximum Sound Pressure Levels (SPL) on a highway occur between 900 and 1000 Hz, making it necessary to seek solutions that can be effective for this frequency range. Morandi et al. [10], showed that, for the frequency range between 600 and 1000 Hz, in SCNB with their elements geometrically distributed in a square shape, the increase in the number of columns in this barrier causes a rise in insertion loss. However, Morandi et al. [10] observed that, after the fourth column of elements, there is no longer a significant increase in sound attenuation. Godinho et al. [11] corroborate the idea of "saturation" from the fourth column onwards of sonic crystal elements.

Besides having a good efficiency when used for the control of road traffic noise, the acoustic sonic crystal barriers can also be built considering a sustainable feature. Godinho et al. [6] and Amado-Mendes et al. [7, 8] studied the use of wood logs from forest cleaning operations as elements of acoustic barriers of sonic crystals.

Despite all the developments in noise barriers in recent years, one interesting way to increase the performance of these solutions can be the coupling of sound-absorbent materials. In Fujiwara et al. [12], it is shown that the attenuation caused by the use of absorbent materials in conjunction with acoustic wall-type barriers can be up to 8 dB.

When a sound-absorbent treatment is required, porous materials can be highlighted. Materials such as fibres and foams are commonly used in commercial acoustic solutions due to their excellent sound absorption behaviour at high frequencies. The work of Pereira et al. [13] studied the sound absorptive behaviour of porous concrete samples made using expanded clay aggregates, and the influence of the grain size, the thickness, and the water ratio in the sound absorption coefficient. In addition, Pereira et al [14] presented the Metaporous Concrete concept, where acoustic resonators were embedded in porous concrete samples. This study was performed using the equivalent-fluid theory to represent each part that composes this solution in finite element models. The present work aims to propose the use of porous concrete materials coating the acoustic sonic crystal barriers. Thus, it is necessary to develop capable numerical models to predict the performance of these noise mitigation solutions.

A challenge in the analysis of sonic crystals is related to its correct, precise and efficient modelling using numerical techniques. A promising approach using the Boundary Element Method (BEM) was presented by Karimi et al. [15], implementing what the authors call Periodic BEM to analyse large matrices of acoustic dispersers periodically distributed. The Finite Element Method (FEM) has also been used, for example, in defining an engineering approach to the sonic crystal barrier design, using overlapping two-dimensional FEM models [16].

In this work, the Method of Fundamental Solutions (MFS) will be applied to predict SCNB covered by porous materials. The MFS can be found in several works over the past two decades. Noteworthy are the works of Fairweather et al. [17] and Golberg and Chen [18]. Despite the simplicity of the method, several works already published indicate that it can provide the calculation of very rigorous solutions for different types of physical problems.

Considering the problems of SCNB, its approach using the FEM would be very laborious, as it requires the discretization of the entire domain. In the case of the BEM, it would require a higher computational cost and the resolution of several integrals along the border. By comparison, MFS does not present these difficulties, making the modelling process simpler. According to Godinho et al. [19], the 2.5-D MFS was used with an Adaptive Cross Approach (ACA) to obtain the sound pressure module for two sonic crystal noise barriers with different heights. In addition to these works, in the papers by Godinho et al. [11] and Veloso et al. [20] the MFS was also used to solve problems involving sonic crystal noise barriers.

In the remaining part of this article, first, the mathematical formulation of the finite 2-D MFS is presented, together with the standard fundamental solutions for infinite and semi-infinite acoustic media. Next the infinite periodic model is then compared with the FEM model and 2-D finite MFS. In the sequence, the granular porous material is integrated in the MFS model using the Horoshenkov-Swift model and this model is also compared with the FEM. Finally, a comparison between two strategies to evaluate the performance of SCNB was done: i) imposing the surface impedance (Z_s) of the absorbent material, at the collocation points of the numerical model; ii) simulating the volume of the absorbent material using equivalent fluid models for porous or granular materials.

2 Mathematical formulation

In this section, the mathematical formulation for the Method of Fundamental Solutions will be presented. In addition, the semi phenomenological model proposed by Horoshenkov and Swift, to represent porous granular materials, will also be described.

2.1 Method of Fundamental Solutions

Meshless methods have been highly developed in the last two decades and among those that stand out the most is the Method of Fundamental Solutions (MFS). By definition, and disregarding some exceptions, meshless methods do not require finite element discretization. Typically, the MFS needs only defined points along the domain boundary. These methods can use high-order interpolation functions or even use differential equations to solve the problem, which significantly increases the method's accuracy. Finally, when the MFS is used, it is not necessary to solve any integral, which sometimes leads to difficulties or increased calculation times. According to Martins et al. [21], the propagation of sound within a 2-D space can be mathematically described, in the frequency domain, by the Helmholtz partial differential equation,

$$\nabla^2 p + \frac{\omega^2}{c^2} p = - \sum_{k=1}^{NS} Q_k \delta(\mathbf{x}_k^f, \mathbf{x}), \quad (1)$$

where $\nabla^2 = \frac{\partial^2}{\partial x^2} + \frac{\partial^2}{\partial y^2}$ is the Laplacian; p is the acoustic pressure; $k = \frac{\omega}{c}$ is the wavenumber of the medium; $\omega = 2\pi f$ is the angular frequency; f is the frequency; c is the speed of sound propagation in the acoustic environment; NS is the number of sources in the domain; Q_k is the magnitude of existing sources \mathbf{x}_k^f located in (x_k^f, y_k^f) ; \mathbf{x} is a field point located at (x, y) ; and $\delta(\mathbf{x}_k^f, \mathbf{x})$ is the Dirac's delta generalized function.

The boundary conditions for the problem (considering a generic point \mathbf{x} in the outline Γ) are given by: $p(\mathbf{x}) = k_d$, $\frac{\partial p(\mathbf{x})}{\partial \mathbf{n}} = k_n$ and $B_1 p(\mathbf{x}) + B_2 \frac{\partial p(\mathbf{x})}{\partial \mathbf{n}} = k_r$ for $\mathbf{x} \in \Gamma$, where k_d , k_n and k_r are the Dirichlet, Neumann and Robin constants, respectively.

Considering that a source point is placed in a generic propagation domain, at $\mathbf{x}_0 (x_0, y_0)$, it is possible to establish the fundamental solution for the incident sound pressure, for the first order derivative of pressure and for the normal particle velocity at a point \mathbf{x} , as suggested by Martins [4], which can be written as:

$$\text{Pressure: } G(\mathbf{x}, \mathbf{x}_0) = -\frac{i}{4} H_0^{(2)}(kr) \quad (2)$$

$$\text{First derivative: } \frac{\partial G(\mathbf{x}, \mathbf{x}_0)}{\partial \mathbf{n}} = H(\mathbf{x}, \mathbf{x}_0, \mathbf{n}) = \frac{i}{4} H_1^{(2)}(kr) \frac{\partial r}{\partial \mathbf{n}} \quad (3)$$

where: G is a type of Green Function, $H_0^{(2)}$ is a Hankel functions of zero order and second kind, $H_1^{(2)}$ is a Hankel functions of first order and second kind and $r = \sqrt{(x - x_0)^2 + (y - y_0)^2}$.

The MFS can be used to calculate the response anywhere in the ω frequency domain. According to the works of Godinho et al [19,11], the solution is obtained with a linear combination of fundamental solutions, using several virtual sources NVS, with amplitude A_l (with $l = 1, \dots, NVS$). These virtual sources are placed outside the domain of interest (i.e., in the case of acoustic barriers, inside the elements of the barrier, since the propagation occurs outside). Thus, the pressure field can be calculated as:

$$p(\mathbf{x}) = \sum_{l=1}^{NVS} [A_l G(\mathbf{x}_l^v, \mathbf{x})] + P_{inc}(\mathbf{x}) \quad (4)$$

where A_l are the unknown amplitudes of the virtual sources, which will be calculated by imposing boundary conditions and G is the fundamental solution at the point \mathbf{x} for the virtual sources located \mathbf{x}_l^v . $P_{inc}(\mathbf{x})$ represents an incident pressure field generated by sound sources present within the domain. In many cases, when the MFS is used, an equal number of placement or collocation points and virtual sources is considered, resulting in a square equation system ($NVS \times NVS$). A generic domain is illustrated schematically in Figure 1.

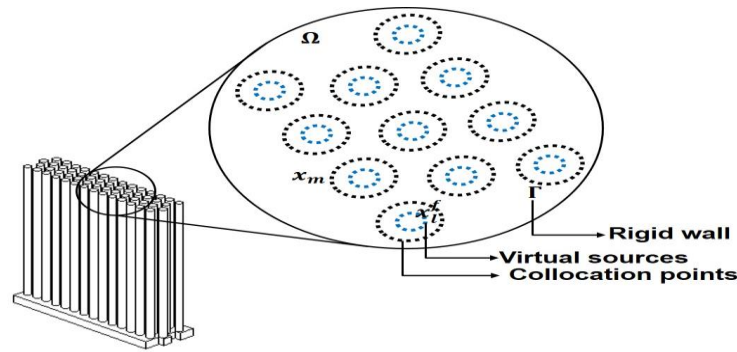


Figure 1 Schematic definition of the collocation points and the virtual sources applied to sonic crystals noise barriers.

This system of equations is constructed by prescribing, at each collocation point \mathbf{x}_m , along the limits of the barrier elements, the correct boundary conditions. When this procedure is applied, the following equations are obtained:

$$\sum_{l=1}^{NVS} A_l \frac{\partial G(\mathbf{x}_l^v, \mathbf{x}_m)}{\partial \mathbf{n}} = - \frac{\partial P_{inc}(\mathbf{x}_m)}{\partial \mathbf{n}} \quad (5)$$

$$\sum_{l=1}^{NVS} [A_l G(\mathbf{x}_l^v, \mathbf{x}_m)] + P_{inc}(\mathbf{x}_m) = i \frac{\bar{Z}}{\rho \omega} \left(\sum_{l=1}^{NVS} A_l \frac{\partial G(\mathbf{x}_l^v, \mathbf{x}_m)}{\partial \mathbf{n}} + \frac{\partial P_{inc}(\mathbf{x}_m)}{\partial \mathbf{n}} \right) \quad (6)$$

Equation (5) describes the case of rigid surfaces, while Equation (6) is employed if absorption is required to be assigned on the model surfaces. For both cases, a resulting $NVS \times NVS$ system of equations can be written, which allows obtaining the acoustic pressure at any point in the domain, by Equation (4).

2.2 MFS extension for problems with more than one region

The formulation previously described allows the analysis of acoustic problems in which there is a domain with multiple embedded scatterers. However, the presented formulation does not allow to analyse some other situations of interest, namely those that correspond to problems with multiple sub-regions or with open elements with thin walls, instead of scatterers.

Considering the generic scheme of Figure 2, in which the domain Ω is divided into two subdomains Ω_1 and Ω_2 , the interface between both also being divided into two parts, one corresponding to the real boundary and the other corresponding to a virtual interface created only for the purposes of numerical modelling (thus making it possible to define a contour line of the interior subdomain according to a regular shape without any edges).

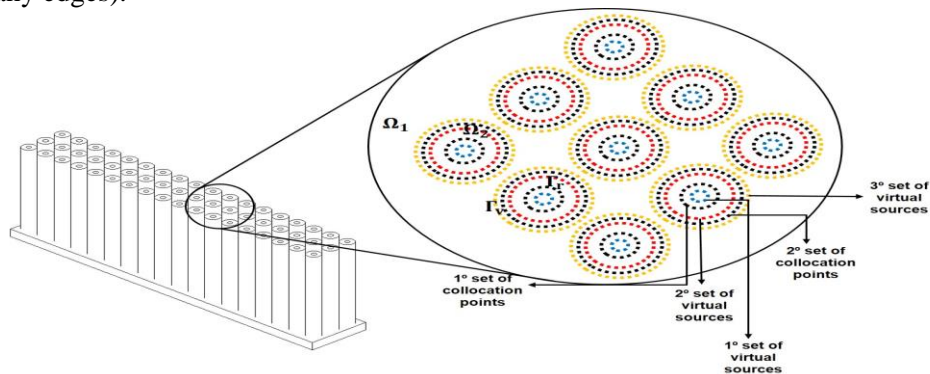


Figure 2 - Schematic definition of the collocation points and the virtual sources applied to sonic crystals acoustic barriers covered by porous concrete.

Considering Figure 2, it is now required to define two sets of virtual sources, each containing NVS virtual sources, that will simulate, respectively, the pressure fields in the outer subdomain, Ω_1 , and in the inner subdomain, Ω_2 , and that are given by

$$p(\mathbf{x}, k_i) = \sum_{l=1}^{NVS} [A_{i,l} G(\mathbf{x}_{i,l}^v, \mathbf{x}, k_i)] \text{ for } \mathbf{x} \in \Omega_i, \quad i = 1, 2 \quad (7)$$

where $A_{1,l}$ and $A_{2,l}$ are the amplitudes of each of the sets of virtual sources, initially unknown. To allow the resolution of this problem, it is also necessary to prescribe the appropriate boundary conditions, along the real boundary and the virtual interface. In the case of the first, along Γ_r , those conditions correspond to the prescription of particle velocity equal to zero in the normal direction to the boundary (imposed either in Ω_1 or Ω_2), while in the second, along Γ_v , it is necessary to impose the continuity of the pressure field and the speed field in the normal direction to the virtual border. Thus, considering NC1 collocation points distributed in Γ_r , and NC2 collocation points distributed Γ_v , in such a way that $NC1 + NC2 = NS$, a system of $2NS$ equations is established with $2NS$ unknowns.

2.3 MFS for infinite periodic system

Herein, the interest is now focused on the analysis of acoustic scattering by infinite sets of elements of a sonic crystals noise barrier. For this scenario, using the fundamental solution described by Equation (2) leads to the need to model each of the scatterers (or set of scatterers) using MFS, distributing placement points and virtual sources associated with each scatterer. To accurately simulate an infinite array, it would be necessary to consider many scatterers to avoid diffraction effects that should not occur for an infinite array.

According to Godinho et al.[11] it is possible to rewrite Equation (4) that determines the pressure value at a point \mathbf{x} of the domain, using the idea of infinite and periodic MFS. Thus, the pressure at a point \mathbf{x} of the domain is calculated as

$$p(\mathbf{x}) = \sum_{l=1}^{NVS_i} \left(A_l \sum_{i=-\infty}^{+\infty} [G(\mathbf{x}_{i,l}^v, \mathbf{x})] \right) + P_{inc}^{per}(\mathbf{x}) \quad (8)$$

In a similar way as an infinite periodic sound pressure was defined, it is also possible to define the Green's function, using the idea of infinite periodicity. Thus, the periodic and infinite Green's function is given by

$$G_{per}(\mathbf{x}_l^v, \mathbf{x}) = \sum_{i=-\infty}^{+\infty} G(\mathbf{x}_{i,l}^v, \mathbf{x}) p(\mathbf{x}) = -\frac{i}{4a} \sum_{-\infty}^{+\infty} (A_l) H_0^{(2)}(k'r') e^{-i \times \frac{2\pi}{a} \times n \times (y-y_0)} \quad (9)$$

where a is the periodicity constant in the yy direction (distance between centre of scatterers).

2.4 Porous Concrete modelled as equivalent fluid

Porous materials are composed of two phases, one solid (skeleton) and the other fluid. Acoustic dissipation within porous materials occurs due to the interaction between the solid and the fluid phases [22, 23], being these losses viscous and/or thermal. The interest in developing porous concrete solutions for external passive noise treatment has increased in the last years because these materials do not require protection against environmental agents and structural reinforcement.

In porous concrete materials, the granules (aggregates) are usually distributed differently from the fibres by following a log-normal pore distribution, resulting in smaller porosity and higher tortuosity [13]. The sound absorption coefficient of porous concrete materials depends on the porous size, the sample thickness and the water-cement ratio.

The Horoshenkov-Swift model considers four macroscopic parameters, namely, the air flow resistivity, σ , the open porosity, ϕ , the tortuosity, α_∞ and the pore size standard deviation, σ_p . The fluid

equivalent properties, the complex density, $\tilde{\rho}$, and the complex compressibility, \tilde{C} , respectively, can be calculated using the following equations:

$$\tilde{\rho}_{\text{eq}} = \frac{\alpha_{\infty}}{\phi} \left(\rho_0 - i \frac{\phi \sigma}{\omega \alpha_{\infty}} \tilde{\mathbf{F}}(\omega) \right) \quad (10)$$

$$\tilde{C}_{\text{eq}} = \frac{\phi}{\gamma P_0} \left(\gamma - \frac{\rho_0 (\gamma - 1)}{\rho_0 - \frac{\sigma \phi}{\omega \alpha_{\infty} N_{\text{Pr}}} \tilde{\mathbf{F}}(N_{\text{Pr}} \omega)} \right) \quad (11)$$

The term γ is the ratio of specific heats, P_0 is the atmospheric pressure, and N_{Pr} is the Prandtl number, and $\tilde{\mathbf{F}}(\omega)$ is the viscosity correction function, which can be presented in the form of a Padé approximation as:

$$\tilde{\mathbf{F}}(\omega) = \frac{1 + a_1 \epsilon + a_2 \epsilon^2}{1 + b_1 \epsilon} \quad (12)$$

Here, $\epsilon = \sqrt{i \frac{\omega \rho_0 \alpha_{\infty}}{\sigma \phi}}$ term is a dimensionless parameter, $a_1 = \frac{\theta_1}{\theta_2}$, $a_2 = \theta_1$, $b_1 = a_1$. The terms θ_1 and θ_2 are pore shape factors defined by the porous geometry. When a circular pore shape is assumed, $\xi = [\sigma_p \ln(2)]^2$, two asymptotic expansion coefficients can be obtained by $\theta_1 = \left(\frac{4}{3}\right) e^{4\xi} - 1$ and $\theta_2 = \left(\frac{1}{\sqrt{2}}\right) e^{\frac{3}{2}\xi}$. The characteristic impedance and the wavenumber of the material are given, respectively, by $\tilde{Z}_c = \sqrt{\tilde{\rho}_{\text{eq}} \tilde{K}_{\text{eq}}}$ and $\tilde{k}_c = \omega \sqrt{\frac{\tilde{\rho}_{\text{eq}}}{\tilde{K}_{\text{eq}}}}$, where $\tilde{\rho}_{\text{eq}}$ is the complex density, \tilde{K}_{eq} is the bulk modulus, and $\tilde{K}_{\text{eq}} = \frac{1}{\tilde{C}}$.

3 Numerical model verification

In this section, the numerical verification of the infinite periodic MFS model is presented against the finite element method. For this, the configurations of rigid sonic crystal barriers and sonic crystal barriers covered with porous concrete will be compared. In the case of porous concrete, two approaches will be used: i) imposing the surface impedance (Z_s) of the absorbent material, at the collocation points of the numerical model; ii) simulating the volume of the absorbent material using granular materials properties.

3.1 Numerical verification of the infinite periodic MFS model considering rigid barriers

The use of the infinite periodic MFS corresponds to a lower computational cost, with this model being verified by comparison with FEM, which can be expressed in the following matrix form [23, 24]:

$$([\mathbf{H}] + i\omega[\mathbf{D}] - \omega^2[\mathbf{Q}])\{\mathbf{p}\} = \{\mathbf{q}\}, \quad (13)$$

where \mathbf{Q} , \mathbf{D} and \mathbf{H} are, respectively, the matrices of inertia, damping and global acoustic stiffness, \mathbf{q} is the nodal excitation vector and \mathbf{p} the acoustic pressure.

The infinite periodic MFS was developed in the context of modelling road traffic noise mitigation measures. For this, a square geometric distribution is considered, using three columns of scatterers and a periodicity/distance between the centre of the circular elements of the noise barrier a equal to 17 cm and the radius of the circular elements equal to 6 cm. The configuration used in the FEM model (which can be seen in Figure 3) consists of representing only one line (or “slice”) of the elements of the sonic crystal noise barrier. However, this is only possible considering symmetrical and periodic geometries.

In Figure 3, it can be seen that the FEM model is represented by a rectangular region, where pressure (in the form of plane waves) is imposed on the left boundary represented by plane waves. Rigid wall boundary conditions ($v = 0$) are considered on the upper and lower boundaries of the rectangle, and on the walls of the circular elements of the barrier, in addition to imposing, at the right end of the rectangular domain, an impedance condition ($Z = \rho_0 c_0$), where ρ_0 is the air density and c_0 is the sound velocity in the

air. As for the mesh, triangular elements with a maximum dimension equal to 2 cm is used (a minimum of 8 elements per wavelength is adopted for a frequency of 2kHz).

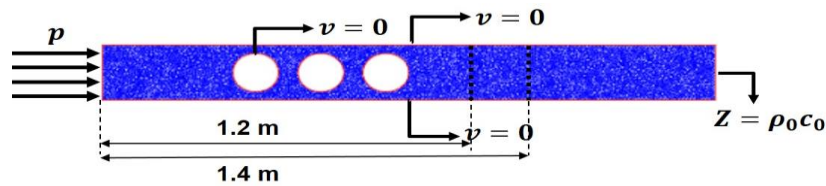


Figure 3 Configuration used in a FEM model representing the periodic sonic crystal noise barrier with rigid scatterers.

To evaluate the IL of the sonic crystal noise barrier, two lines of receivers (positioned at 1.2 and 1.4 m from the line source) are used. The result obtained by the FEM is used to verify the result of the infinite periodic MFS model. The comparison between the results of infinite periodic FEM, the infinite periodic MFS and the finite MFS can be observed in Figure 4.

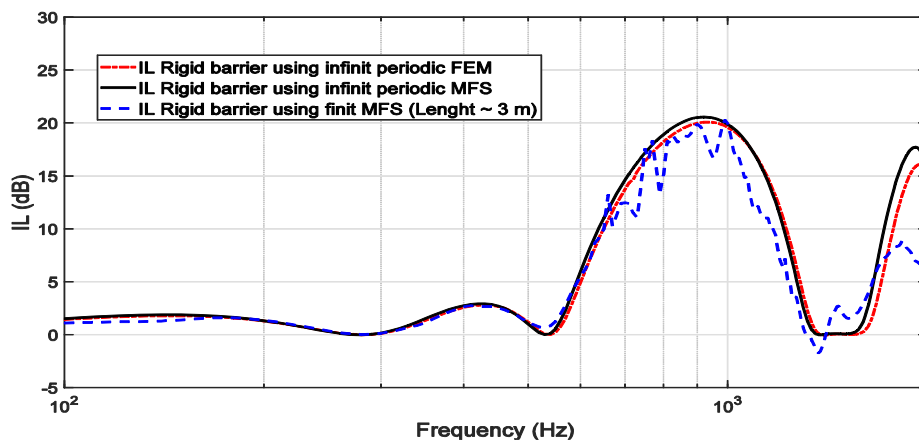


Figure 4 - Comparison of IL results for SCNB using the FEM model, infinite periodic MFS and finite MFS.

When analyzing the result presented in Figure 4 it is possible to observe that all approaches (FEM, infinite periodic MFS and finite MFS) present, in general, a satisfactory representation of the insertion loss for a sonic crystal noise barrier. With all numerical models it is possible to assess that the bandgap is well represented, with IL amplitude presenting the same order of magnitude when analyzing the first peak and a small difference for the second peak.

3.2 Verification of the MFS considering acoustic barriers covered by porous materials

To evaluate the use of porous concrete applied to sonic crystal noise barriers in order to mitigate the road traffic noise, two numerical approaches are applied in conjunction with the MFS model. These approaches will represent porous concrete either as a surface impedance condition applied in the collocation points, or as an equivalent fluid strategy using the Horoshenkov-Swift model to define the complex properties. In Figure 5, an illustrative scheme is presented of the infinite periodic and multilayer MFS model used to represent the sonic crystals noise barriers. In this model, the value of the external radius (r_2) is set to 6 cm and the thickness of the porous material is modified (e), and the internal radius (r_1) is given by $r_1 = r_2 - e$. Two types of boundaries were considered, the first being rigid and the other with conditions of continuity of pressure and particle velocity imposed between the Ω_1 and Ω_2 domains.

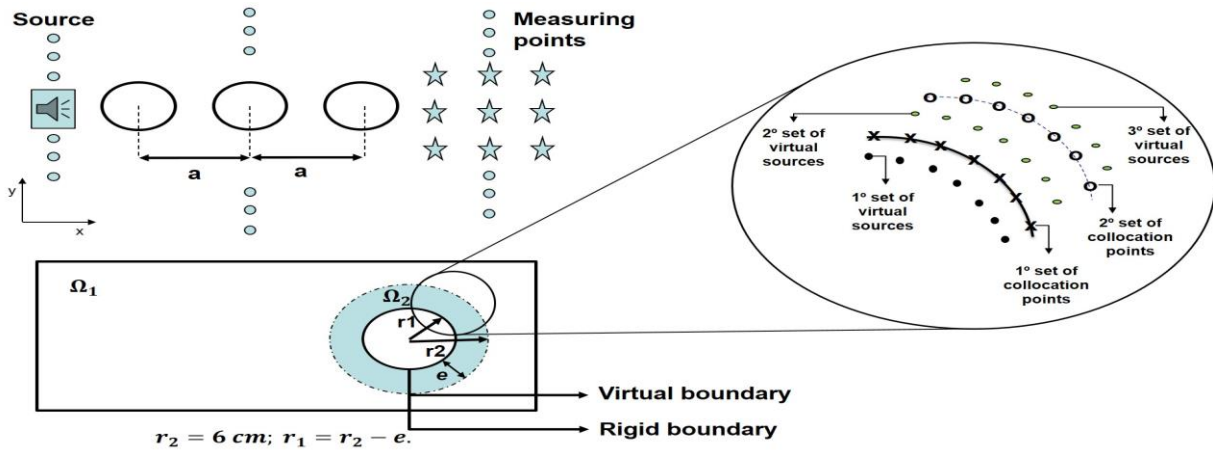


Figure 5 - Schematic illustration of the MFS model of the SCNB covered by porous concrete.

Herein, the porous concrete is represented by an equivalent fluid, using the equations presented in Section 2.4. The four macroscopic parameters used to describe the porous concrete made with expanded clay aggregates were previously obtained in [14], with these parameters being obtained through an inversion technique, except the open porosity, that was experimentally characterized. These parameters are presented in Table 1.

Table 1 Macroscopic parameters obtained for the porous concrete samples.

	Airflow resistivity σ [Ns/m^4]	Open porosity ϕ [-]	Tortuosity α_∞ [-]	Standard deviation of the pore size σ_p [-]
M2	3896.06	0.46	1.89	0.25
M3	7171.53	0.36	2.73	0.41

After obtaining the macroscopic parameters, the M2 mixture is used to cover the sonic crystal noise barriers elements and this configuration is simulated using the infinite periodic MFS model, as illustrated in Figure 5. This model is verified using the FEM model as in the previous section. In addition, the infinite periodic MFS with the Z_s imposed in the collocation points to represent the effect of porous concrete was also the verified, which was done by comparing with the FEM model results and an identical configuration.

The only difference between the FEM model presented in Figure 3 and the FEM with porous concrete is that, in the last one, a region with thickness (e) with greater discretization was created where the equivalent fluid properties, obtained through the Horoshenkov-Swift model, were ascribed (similarly to Figure 5) and the obtained results can be seen in Figure 6.

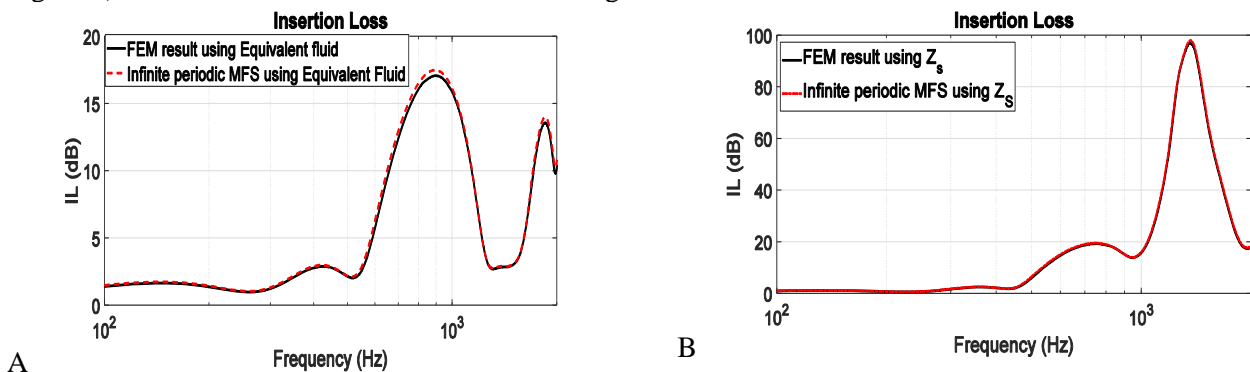


Figure 6 Comparison of IL results for the absorbing SCNB using two approaches: (A) modelling the porous concrete as an equivalent fluid; and (B) imposing Z_s of the porous concrete, at the collocation points.

Figure 6 shows the comparison of the results of the insertion loss of sonic crystal noise barriers using the infinite periodic MFS model and the FEM model. In this figure, it is possible to observe that both models have the same aspect throughout the analysed frequency spectrum although different approaches are followed; in addition, the bandgap is well represented in both approaches. Thus, it is possible to conclude that the infinite periodic MFS model has been satisfactorily verified.

4 Comparison of approaches using Z_s and equivalent fluids

After the verification of the MFS model using equivalent fluids and surface impedance (Z_s) to represent the porous concrete, it was decided to compare the two approaches using the M3 mixture of porous concrete with the properties presented in Table 1. The result of the comparison between these two approaches can be seen in Figure 7.

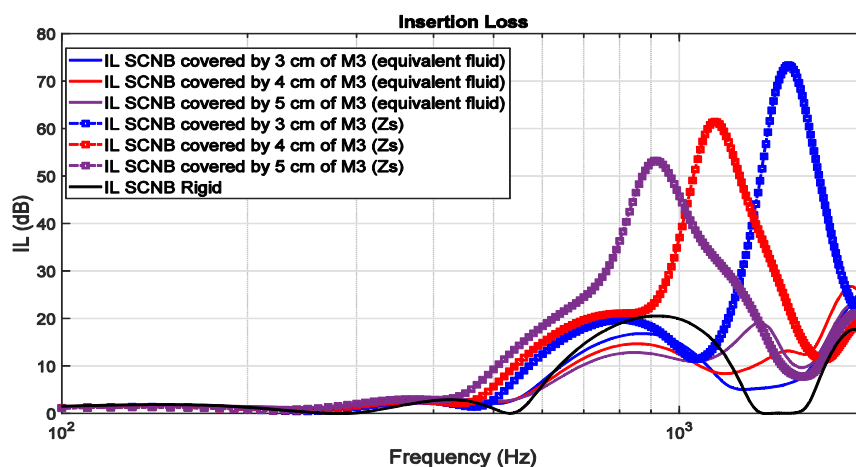


Figure 7 - Comparison of IL results for the SCNB covered by porous concrete using Z_s and fluid equivalent model.

In Figure 7, the comparison of IL results for SCNB covered with porous concrete is presented making use of two approaches: i) prescription of the surface impedance (Z_s) of the absorbent material, at the collocation points of the numerical model; ii) simulation of the volume of the absorbent material using granular materials. Analysing the results of Figure 7 it is possible to observe that, in the cases where Z_s was used, a much larger IL was obtained than in the cases where the porous concrete was modelled as an equivalent fluid.

Furthermore, in all cases where Z_s is used, the result of IL is greater along the entire frequency spectrum when compared to rigid SCNB. When comparing the IL for rigid SCNB with the SCNB covered by porous concrete modelled by equivalent fluid, it can be seen that the rigid barrier presents a higher IL in the bandgap and the SCNB with absorbent material has a higher IL right after the bandgap. Finally, it is possible to observe that, for both approaches, the bandgap is slightly shifted to lower frequencies.

5 Conclusions

In this work, the authors present the comparison of two numerical approaches, using the MFS, capable of simulating the IL of SCNB covered by sound absorbent porous concrete. First, to use these approaches, a verification of the MFS models was achieved by comparing with FEM was performed. With the verification of the numerical models, a good correlation between the MFS and FEM it was possible to observe along the entire frequency spectrum, and the bandgap was well represented in both models.

Finally, a comparison was made of the use of Z_s and equivalent fluids to represent the effects of SCNB coated porous concrete. In these results, it was possible to observe that when using Z_s there is an IL several

times greater than when using the equivalent fluid model, however, it is believed that the results obtained through the prescription of Zs in a set of collocation points are unrealistic. On the other hand, the results obtained through the equivalent fluid model are quite consistent, as a decrease in the magnitude of the bandgap can be seen depending on the thickness of material used, as it is believed that the use of these materials interfere with the Bragg effect, however, with the use of porous concrete, an increase in IL is observed right after the bandgap.

Acknowledgements

This work was developed within the scope of the project with reference POCI-01-0247-FEDER-033691 – HLS - Hybrid Log Shield, supported by FEDER funds, through Portugal-2020 (PT2020) Programme, within the scope of SII&DT System, and by POCI Programme. This work has been partly financed by national funds through FCT – Foundation for Science and Technology, I.P., within the scope of the R&D unit Institute for Sustainability and Innovation in Structural Engineering - ISISE (UIDP/04029/2020) and through the Regional Operational Programme CENTRO2020 within the scope of the project CENTRO-01-0145-FEDER-000006 (SUSPENSãoE).

FCT Fundação para a Ciência e a Tecnologia

MINISTÉRIO DA CIÊNCIA, TECNOLOGIA E ENSINO SUPERIOR

References

- [1] Gill, H. (1983). Efficacy of barriers on propagation of construction noise. *The journal of the Acoustical Society of America*, 73(2), 699-700.
- [2] Hutchins, D., Jones, H. & Russell, L. (1984). Model studies of barrier performance in the presence of ground surfaces. Part ii – different shapes. *The journal of the Acoustical Society of America*, 75(6), 1817-1826.
- [3] Bies, D. A., Hansen, C., Howard, C. (2017). *Engineering noise control: Theory and Practice*, 4th Edition, CRC press.
- [4] Martins, M. M. d. A. (2015). *Contribuição para o estudo da atenuação seletiva do ruído de tráfego rodoviário*. Tese de doutoramento, Universidade de Coimbra, Portugal
- [5] Fredianelli, L., Del Pizzo, A. & Licitra, G. (2019). Recent developments in sonic crystals as barriers for road traffic noise mitigation. *Environments*, 6(2), 14.
- [6] Godinho, L., Santos, P. G., Amado-Mendes, P., Pereira, A. & Martins, M. (2016). Experimental and numerical analysis of sustainable sonic crystals barriers based on timber logs. *Proceedings of the EuroRegion, Porto, Portugal*, 13-15.
- [7] Amado-Mendes, P., Godinho, L., Santos, P., Dias, A., Santos, P. et al. (2015). On the use of periodic arrays of timber logs as a sustainable noise mitigation solution. *Proceedings of ICSV22, Florence, Italy*.
- [8] Amado-Mendes, P., Godinho, L., Santos, P., Dias, A. & Martins, M. (2016). Laboratory and full-scale experimental evaluation of the acoustic behaviour of sonic crystals noise barriers. *Proceedings of the 22nd International Congress on Acoustics (ICA 2016), Buenos Aires, Argentina*.
- [9] Martínez-Sala, R., Sancho, J. & S. J. G. V. L. J. M. F. (1995). Sound attenuation by sculpture. *Nature*, 378, 241.
- [10] Morandi, F., Miniaci, M., Marzani, A., Barbaresi, L. & Garai, M. (2016). Standardised acoustic characterisation of sonic crystals noise barriers: Sound insulation and reflection properties. *Applied Acoustics*, 144, 294 – 306.

- [11] Godinho, L., Redondo, J. & Amado-Mendes, P. (2019). The method of fundamental solutions for the analysis of infinite 3D sonic crystals. *Engineering Analysis with Boundary Elements*, 98, 172 – 183.
- [12] Fujuwara, K., Ando, Y., Maekawa, Z. (1977). Noise control by barriers – part 2: noise reduction by an absorptive barrier. *Applied Acoustics*, 10, 167 – 179.
- [13] Pereira, M., Carbajo, J., Godinho, L., Amado-Mendes, P., Mateus, D., Ramis-Soriano, J. (2019). Acoustic behavior of porous concrete - Characterization by experimentals and inversion methods. *Construction and Building Materials*, 69(336).
- [14] Pereira, M., Carbajo, J., Godinho, L., Ramis-Soriano, J., Amado-Mendes, P. (2021). Improving the sound absorption behavior of porous concrete using embedded resonant structures, *Journal of Building Engineering*, 35.
- [15] Karimi, M., Croaker, P., Kessissoglou, N. (2016). Boundary element solution for periodic acoustic problems, *Journal of Sound and vibration*, 360, 129 – 139.
- [16] Castiñeira-Ibáñez, S., Rubio, C., Sánchez-Pérez, J.V. (2013). Acoustic wave diffraction at the upper edge of a two-dimensional periodic array of finite rigid cylinders. A comprehensive desing model of periodicity-based devices, *EPL (Europhysics Letters)*, 101(6).
- [17] Fairweather, G., Karageorghis, A. & Martins, P. A. (2003). The method of fundamental solutions for scattering and radiation problems. *Engineering Analysis with Boundary Elements*. 27(7), 759 – 769.
- [18] Golberg, M., Chen, C. (1998). The method of fundamental solutions for potential, Helmholtz and diffusion problems, *Boundary Integral Methods: numerical and mathematical aspects 1*, 103 – 176.
- [19] Godinho, L., Sores Jr, D., & Santos, P. (2016). Efficient analysis of sound propagation in sonic crystals using an ACA-MFS approach. *Engineering Analysis with Boundary Elements*. 69, 72 – 85.
- [20] Veloso, M., Godinho, L., Amado-Mendes, P. & Redondo, J. (2020). Avaliação das perdas viscotérmicas usando o método das soluções fundamentais. *Proceedings of XI Congresso Ibérico de Acústica. 51º Congresso Espanhol de Acústica TECNIACUSTICA 2020*.
- [21] Martins, M., Godinho, L. & Picado-Santos, L. (2013). Numerical evaluation of sound attenuation provided by periodic structures. *Archives of Acoustical*, 38(4), 503 – 516.
- [22] Allard, J., Atalla, N. (2009). *Propagation of Sound in Porous Media: Modeling Sound Absorbing Materials*. 2nd Edition. Wiley.
- [23] Mareze, P. H. (2013). *Análise da influência da microgeometria na absorção sonora de materiais porosos de estrutura rígida*. Tese de Doutorado em Engenharia Mecânica. Universidade Federal de Santa Catarina. Florianópolis.
- [24] Bermúdez, A., Ferrin, J., Prieto, A. (2005). A finite element solution of acoustic propagation in rigid porous media. *International Journal for numerical methods in engineering*, 62(10), 1295 – 1314.